Estuaries Vol. 26, No. 2A, p. 298–309 April 2003

Effect of Nutrient Loading on Atlantic Menhaden (*Brevoortia tyrannus*) Growth Rate Potential in the Patuxent River

STEPHEN B. BRANDT* and DORAN M. MASON

National Oceanic and Atmospheric Administration, Great Lakes Environmental Research Laboratory, 2205 Commonwealth Boulevard, Ann Arbor, Michigan 48105

ABSTRACT: We linked a 2-dimensional water quality model of the Patuxent River with a spatially-explicit model of fish growth to simulate how changes in land use in the Patuxent River Basin would affect the growth rate potential (GRP) of Atlantic menhaden (*Brevoortia tyrannus*). Simulations of three land-use patterns that reflected current nutrient loadings, increased nutrient loadings, and decreased nutrient loadings were used to drive the water quality model. Changes in nutrient loadings caused changes in the timing and intensity of phytoplankton concentrations and the region of hypoxia increased during summer with increased nutrient loading. The spatial distribution of menhaden GRP was highly correlated with phytoplankton concentrations and localized in the middle one third of the Patuxent River. Menhaden growth rate was highest in early June and late summer. During June, menhaden GRP (and phytoplankton concentration) was lowest at the lower nutrient loading simulation. During late summer, mean menhaden growth rates were inversely proportional to nutrient loading rates and menhaden grew best when nutrient loadings were the lowest. Upriver to mid-river phytoplankton patches drove overall mean calculations. Model results suggest that more research is needed on water quality model predictions of phytoplankton levels at a high level of spatial and temporal resolution, menhaden foraging, and menhaden habitat selection.

Introduction

The Patuxent River is located in the Chesapeake Bay watershed and is a tributary to the Chesapeake Bay. This estuary is characterized by high nutrient loading, low dissolved oxygen levels below the pycnocline in the mesohaline portion of the river during summer, and high phytoplankton levels in the upper estuary at certain times of the year (D'Elia et al. 2003). Changes in land-use patterns will affect the rates of flow as well as the concentration of nutrients that reach the Patuxent River. The impact of nutrient loadings on such an ecosystem can be large and complex and can cause changes in the timing and spacing of ecosystem production dynamics (Nixon 1981). Most water quality models that simulate these changes in estuaries have not made ecological predictions at trophic levels higher than phytoplankton.

Atlantic menhaden (*Brevoortia tyrannus*) inhabit the Patuxent River and are one of the most abundant pelagic fishes in the Chesapeake Bay ecosystem (U.S. National Marine Fisheries Service [NMFS] 1978; Ahrenholz et al. 1987). Menhaden provide a fundamental link in the Chesapeake Bay food web. Phytoplankton is consumed by filter feeding juveniles (June and Carlson 1971; Durbin and Durbin 1975, 1981; Friedland et al. 1984; Lewis and Peters 1984; Peter and Schaaf 1991; Rippetoe 1993), which, in turn, are one of the primary prey of commercially and recreationally important piscivores such as the striped bass (*Morone saxatilis*), bluefish (*Pomatomus saltatrix*), and weakfish (*Cynoscion regalis*; Hartman and Brandt 1995). Menhaden also provide a direct link between primary production and fisheries. Menhaden are fished commercially in Chesapeake Bay and nearshore habitats of the eastern United States (NMFS 1978; Lewis and Peters 1984) and account for nearly half the total east coast commercial fishery harvest by weight (Peters and Schaaf 1991). Catches of menhaden in the Chesapeake Bay account for more than half of the total commercial catch (Smith 1999).

Menhaden are an estuarine-dependent species and the Chesapeake Bay is a primary nursery ground for juvenile menhaden (Hildebrand and Schroeder 1928). Larval menhaden are spawned in coastal waters in late fall and winter and enter Chesapeake Bay in winter and spring (Warlen 1994). The subsequent growth rates and production of juveniles in the Chesapeake Bay during summer and early fall is a critical stage in menhaden life history and is dependent on prevailing water temperatures and food availability (e.g., Quinlan and Crowder 1999).

Luo et al. (2001) examined the spatial and temporal dynamics of menhaden growth rate potential (GRP) and carrying capacity by linking a spatially-explicit menhaden growth model to the 3-dimen-

* Corresponding author; tele: 734/741-2244; fax: 734/741-2003; e-mail: Stephen.B.Brandt@noaa.gov.

sional water quality model for the Chesapeake Bay (Cerco and Cole 1993). The main object of our research was to simulate how changes in land-use patterns in the Patuxent River watershed might influence the spatial and temporal patterns in GRP and carrying capacity of Atlantic menhaden in the Patuxent River. We use results from a watershed model to drive a water quality model under low, medium (baseline), and high nutrient loadings. We use a spatially-explicit bioenergetics model of menhaden to examine how resultant changes in oxygen levels and phytoplankton concentrations might affect the spatial and temporal patterns in menhaden GRP and carrying capacity.

Materials and Methods

General Approach

We used a combination of a watershed model, a water quality model, menhaden foraging model, and spatially-explicit menhaden bioenergetics model to examine how changes in nutrient loadings to the Patuxent River might affect the spatial and temporal dynamics of GRP and carrying capacity for menhaden. The watershed model and water quality model and their linkages are described elsewhere in this issue (Cronin and Vann 2003; Jordan et al. 2003; Lung and Bai 2003; Weller et al. 2003). We selected land-use patterns that approximated current (baseline) nutrient loadings, as well as higher and lower nutrient loadings, in order to examine how these changes might affect menhaden growth rates and carrying capacity during summer and early fall (June 1 to October 1). The water quality model provided information on the spatial and temporal (daily) patterns in water temperature, salinity, dissolved oxygen concentrations, and phytoplankton biomass density. This information was used to simulate menhaden GRP on a daily basis for low, medium, and high nutrient loadings. Each of these models is briefly described below.

Watershed Model

Freshwater flows into the upper portions of the estuary have significant impacts on the hydrodynamics, nutrient mixing, and phytoplankton production (Lung and Bai 2003). Simulations of three land cover patterns were used to drive the water quality model. The watershed model and its assumptions are described in Weller et al. (2003). The watershed model simulates how changes in land-use patterns (applied uniformly throughout the watershed) change nutrient discharges from the Patuxent River watershed. We refer to the nutrient loadings from these models as low, medium (baseline), and high. The lowered nutrient loading simulation halved the areas of cropland, developed land, and nutrients from point sources. Baseline conditions were considered to be from August 1997 to July 1998. The increased (high) nutrient loading scenario doubled the areas of developed land and doubled the nutrient inputs from point sources. Scenario predictions are expressed as ratios to the baseline (1997–1998) conditions (Weller et al. 2003). In the lowered nutrient loading scenario, all nutrient loadings decreased. Ratios (simulations:baseline) varied from 0.46 for NO_3 to 0.52 for total nitrogen to 0.55 for total phosphorus to 0.86 for silicate. In the high loading scenario, all nutrient concentrations increased except silicate. Ratios (simulations:baseline) varied from 1.16 for organic carbon to 1.24 for total phosphorus to 1.35 to total nitrogen to 1.42 for NO_3. In the lowered nutrient loading scenario, overall flow rates to the Patuxent River were reduced to 96% of baseline conditions. The changes in land use for the higher nutrient loading scenario increased overall flow rates to 108% of baseline conditions (Weller et al. 2003).

2-Dimensional Water Quality Model

The 2-dimensional water quality model and its assumptions are fully described in Lung and Bai (2003) and Cole and Wells (2000). The modeling framework CE-QUAL-W2 (called W2) is 2-dimensional (water depth and distance along the axial transect of the Patuxent River). The model cells represent distance down the Patuxent River by depth in the water column. The total distance covered by the model was 100 km and cell segments were each 613 m in length. The model cross-section spanned the distance from near the Maryland Route 50 bridge (water quality monitoring station PXT0603) to near the mouth of the river (water quality monitoring station XCF8747) as shown in Fig. 1 and described in Table 1 of Lung and Bai (2003). The water column was divided into 1-m intervals and ranged to depths of 34 m. Total number of cells was 1,993 by day and 239,160 cells overall for the 120 days of the model.

The W2 model simulates vertical and longitudinal flow (velocities) and can simulate 21 constituents (Lung and Bai 2003). Flow rates and nutrient loads are input into the water quality model from the land-use watershed model. The principal outputs for the purposes of calculating menhaden GRP were water temperature, salinity, dissolved oxygen levels, and phytoplankton biomass concentration. Temperature conditions were assumed identical for all model simulations. Lung and Bai (2003) calibrated the model with data from 1997 to 1998 by matching results with measured temperature, dissolved oxygen, chlorophyll, and nutrient levels in the water column. Lung and Bai

(2003) have shown that halving the nutrient loads to the estuary had little impact on dissolved oxygen, but increasing the loads caused further increases in the degree of hypoxia. The total modeled time frame for menhaden growth simulations was from June 1 to October 1 in the same calendar year. The water quality model was run from August 1 through July 31 the following year. The first 14 d of the model output were not included in our analyses because it took this long for the model to reach equilibrium. We assumed a linear change in conditions across these 2 wk. For comparisons across space, we selected June 8, July 13, and September 18 because these dates corresponded to dates selected for model validation in Lung and Bai (2003).

Spatially-explicit Foraging and Bioenergetic Models

Spatially-explicit models of fish GRP have been used for a variety of purposes, and, in particular, for comparing the habitat quality afforded by the environment for fish growth. The general approach is more fully described in Brandt et al. (1992), Brandt and Kirsch (1993), and Luo et al. (2001). The aquatic habitat is divided up into spatial cells (depth by location) that are each assumed to be homogeneous over the course of the model run. Each cell is characterized by a specific set of attributes such as water temperature, prey (algal) biomass density, salinity, and dissolved oxygen concentration. GRP is defined as the growth rate that a particular size and type of fish would attain if placed in that cell for a specific unit of time. In our simulations, we assumed a daily time step and water quality model output that was averaged down the river at 4 segment intervals (to 2.45-km lengths and 1-m depth intervals). Habitat conditions within each cell were assumed constant for the duration of the time step and we assumed that fish predation did not change the prey (phytoplankton) biomass concentration.

For each day of the simulation and for each cell we ran process-oriented foraging (consumption) and growth models of the same model structure for menhaden. Principal equations and model parameters used in the model are given in Tables 1 and 2. Further details on model structure, parameters, and approach can be found in Luo et al. (2001). Menhaden were assumed to be 50 mm (1 g) in size at the beginning of the model run on June 1 (Luo et al. 2001). The model was run from June 1 to October 1.

The consumption rate of a filter-feeding menhaden (consumption model, Table 1) was calculated as the product of the algal concentration, menhaden gill-raker filtering efficiency, menhaden

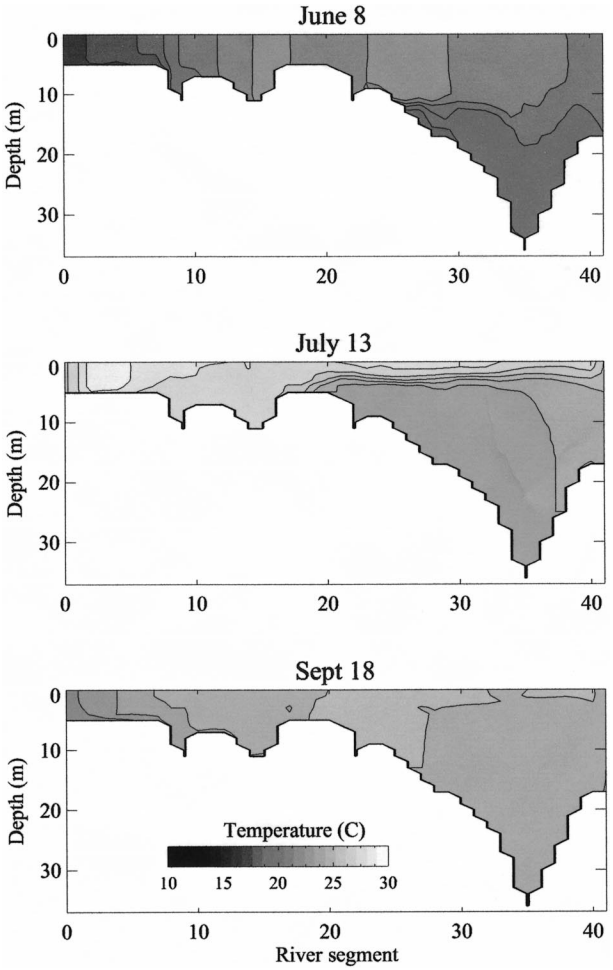

Fig. 1. Two-dimensional spatial distribution of water temperature down the axis of the Patuxent River on June 8, July 13, and September 18.

mouth gape size, and menhaden swimming speed (Rippetoe 1993; Luo et al. 2001). Menhaden of 50 mm or larger are considered to filter-feed on phytoplankton (Friedland et al. 1984; Rippetoe 1993), but their efficiency of retaining phytoplankton increases to about 50% as menhaden grow and gill rakers develop. We modeled this changing efficiency as a sigmoid response curve (see Table 1) as done by Luo et al. (2001). Menhaden gape size is a function of menhaden size, and menhaden swimming speed was considered a function of menhaden size and water temperature (Tables 1 and 2). We modified consumption using a dissolved oxygen dependent scaling function as in Luo et al. (2001; Tables 1 and 2) that is near 0 at 0 mg l^{-1}, is 0.5 at 3 mg l^{-1}, and approaches 1.0 above 4 mg l^{-1}.

Menhaden daily growth rate was calculated using the basic Wisconsin bioenergetics model (Kitchell

TABLE 1. Model equations used for this manuscript. Model is from Lou et al. (2001). See Table 2 for definitions of symbols.

Equation	Description
$GRP = C - (R + SDA + F + U)$	Growth rate potential (g g^{-1} d^{-1})
$\frac{Cons}{wt} = phy \times gap \times u \times eff \times f(DO)$	Consumption (g g^{-1} d^{-1})
phy	Phytoplankton concentration (g m^{-3})
$gap = 2.586E^{-8}TL^{1.798}$	Mouth open area (m^2)
$u = \frac{216 \times TL}{e^{-0.398T+6.378}}$	Swimming velocity (m d^{-1})
$eff = \frac{0.5}{1 + e^{-0.0528TL+2.970}}$	Filtration retention efficiency (dimensionless)
$f(DO) = \frac{1}{1 + e^{-2.197DO+6.592}}$	Dissolved oxygen dependent scale function (dimensionless)
$C_{max} = Ca\ wt^{Cb} f_C(T)$	Maximum consumption (g g^{-1} d^{-1})
$f_C(T) = K_A K_B$	Temperature dependent function from Thorton and Lessem 1978 (dimensionless)
$K_A = \frac{K1e^{y1(T-T1)}}{1 + k1[e^{y1(T-T1)} - 1]}$	
$y1 = \frac{1}{T2 - T1}\ln\left[\frac{K2(1 - K1)}{K1(1 - K2)}\right]$	
$K_B = \frac{K4e^{y2(T4-T)}}{1 + k4[e^{y2(T4-T)} - 1]}$	
$y2 = \frac{1}{T4 - T3}\ln\left[\frac{K3(1 - K4)}{K4(1 - K3)}\right]$	
$C = \min\left\{\frac{Cons}{wt}, C_{max}\right\}$	Adjusted consumption (g g^{-1} d^{-1})
$R = Ra\ wt^{Rb} f_R(T) ACT$	Respiration (g g^{-1} d^{-1})
$f_R(T) = V^x e^{x(1-V)}$	Temperature dependent function (dimensionless)
$V = \frac{RTM - T}{RTM - RTO}$	
$x = \left\{Z^2\left[1 + \left(1 + \frac{40}{Y}\right)^{0.5}\right]^2\right\}\frac{1}{400}$	
$Z = \ln(RQ)(RTM - RTO)$	
$Y = \ln(RQ)(RTM - RTO + 2)$	
$ACT = 1 + \left(\frac{2.5}{1 + e^{-0.398T+6.378}}\right)$	Temperature dependence of activity multiplier (dimensionless)
$S = SDA(C - F)$	Specific dynamic action (g g^{-1} d^{-1})
$F = F_a C$	Egestion (g g^{-1} d^{-1})
$U = U_a(C - F)$	Excretion (g g^{-1} d^{-1})
$CC = \frac{f_p \times phy}{C} \times f(G)$	Carrying capacity (g m^{-3})
$f(G) = \frac{1}{1 + e^{-1358.5GRP+4.6}}$	Growth rate dependent scale function (dimensionless)

et al. 1977; Brandt and Hartman 1993; Hartman and Brandt 1995). The bioenergetics model calculated growth rate (g g^{-1} d^{-1}) of an individual fish of a given size as a balance between energy intake and energy expenditure derived from the prevailing conditions in each cell using the equations and parameters in Tables 1 and 2. We assumed that menhaden would not occupy freshwater and set the GRP at 0 for all freshwater cells for each day. The result is the GRP of the fish had it occupied that particular cell. We calculated carrying capacity following Luo et al. (2001). We assumed within any cell, that 10% of the phytoplankton were consumed and transformed into menhaden growth. The 10% value was that assumed by Luo et al. (2001) for Chesapeake Bay as a whole, based on the rationale that the literature suggests 50–80% of phytoplankton production is consumed by other

TABLE 2. Atlantic menhaden bioenergetics model parameters (Rippetoe 1993; Lou et al. 2001). For model equations, see Table 1.

Symbol	Description	Value	Unit
	Parameters		
Ca	Intercept for C_{max}	1.294	g g^{-1} d^{-1}
Cb	Exponent for C_{max}	−0.312	—
K1	Proportion of C_{max} at T_1	0.525	—
K2	Proportion of C_{max} at T_2	0.980	—
K3	Proportion of C_{max} at T_3	0.980	—
K4	Proportion of C_{max} at T_4	0.810	—
T1	Temperature for K_1	18.2	°C
T2	Temperature for K_2	28.0	°C
T3	Temperature for K_3	29.0	°C
T4	Temperature for K_4	30.1	°C
Ra	Intercept for maximum standard respiration	0.003301	g O_2 g^{-1} d^{-1}
Rb	Exponent for maximum standard respiration	−0.2246	—
RQ	Slope for temperature dependence of standard respiration	2.07	—
RTO	Optimum temperature for standard respiration	33.0	°C
RTM	Maximum temperature for standard respiration	36.0	°C
SDA	Specific dynamic action coefficient	0.172	—
F_a	Proportion of consumed food egested	0.14	—
U_a	Proportion of assimilated food excreted	0.10	—
f_p	Proportion of phytoplankton available to menhaden	0.10*	—
	Variables		
DO	Dissolved oxygen concentration		mg l^{-1}
TL	Menhaden total length		mm
Phy	Phytoplankton biomass concentration		g m^{-3}
T	Water temperature		°C
Wt	Mass		g

* Explained in Lou et al. (2001).

grazers (Baird and Ulanowicz 1989). The 10% value is considered conservative. Carrying capacity was calculated as the total biomass the habitat could support on a given day (see Tables 1 and 2). Additional assumptions for the menhaden model are discussed in Luo et al. (2001), and a sensitivity analysis of the general bioenergetics model is provided by Bartell et al. (1986).

Results

Temperature and Dissolved Oxygen

Mean temperatures were near 21°C in early June and rose to a maximum of 27.5°C in August and were about 20°C in September. The two dimensional spatial distributions of water temperature down the axis of the Patuxent River on June 8, July 13, and September 18 are shown in Fig. 1. During June, water temperatures (total range 16–22°C) were highest in the midsections of the river and largely uniform through the water column in shallower areas. There was only a slight thermal gradient in the deeper parts of the water column. On July 13, water temperatures (total range 22–29°C) were highest in the upper river and lowest in the deeper parts of the water column downriver. There was a thermal gradient in the lower half of the river. On September 18, water temperatures (total range 21–24°C) were largely uniform throughout the water column and slightly cooler in the very upper segments of the river.

The two dimensional spatial distribution of dissolved oxygen on June 8, July 13, and September 18 down the axis of the Patuxent River during low, baseline, and high nutrient loading are shown in Fig. 2. The proportions of the water less than 3 mg l^{-1} within the Patuxent River during low, baseline, and high nutrient loadings across time are given in Fig. 3. Throughout the year, the proportion of water with dissolved oxygen concentrations less than 3 mg l^{-1} increased with increased nutrient loading. During June, oxygen concentrations were reduced below the pycnocline during all three simulations, but more so during the baseline and high nutrient loadings (Fig. 2). Oxygen depletion was most severe during July and August, particularly under the baseline and high nutrient loadings when nearly half of the water column had dissolved oxygen concentrations less than 3 mg l^{-1} (Figs. 2 and 3). Near-bottom oxygen concentrations were below 3 mg l^{-1} over a large distance for the baseline and high nutrient loadings. In contrast, for low nutrient loadings, near-bottom oxygen concentrations were below 3 mg l^{-1} over only a short distance. On September 18, the largest area of lowered oxygen concentrations occurred under high nutrient loadings when about 25% of the total

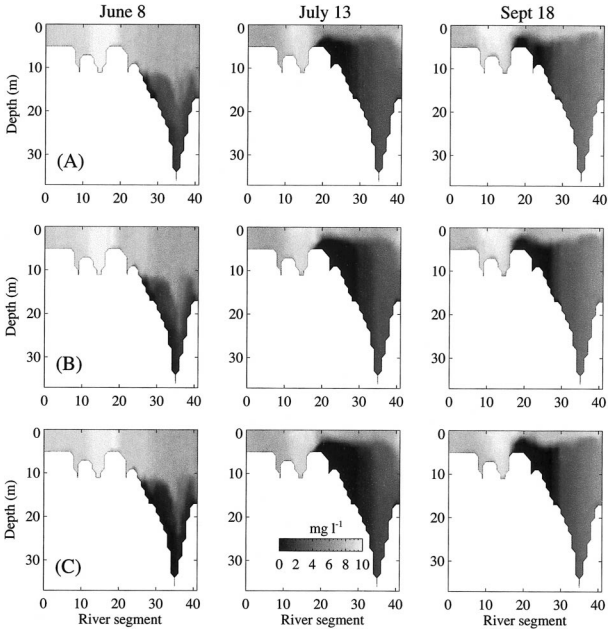

Fig. 2. Two-dimensional spatial distribution of dissolved oxygen on June 8, July 13, and September 18 down the axis of the Patuxent River during low (top row), baseline (middle row), and high (bottom row) nutrient loading.

number of cells had oxygen concentrations less than 3 mg l^{-1} as compared to about 13–16% under low and baseline nutrient loading (Fig. 3).

Phytoplankton

The riverwide mean phytoplankton concentrations across the year under low, baseline, and high nutrient loadings are shown in Fig. 4. Phytoplankton concentrations were highest during the first half of June and during late August. During June, the highest concentration of phytoplankton increased with increased nutrient loading. By July, the overall mean phytoplankton levels as well as highest concentrations occurred at baseline nutrient loading levels. By late August, overall mean phytoplankton densities were inversely related to nutrient loading levels. The 2-dimensional spatial distribution of phytoplankton concentrations on June 8, July 13, and September 18 down the axis of the Patuxent River during low, baseline, and high nutrient loadings are shown in Fig. 5. Phytoplankton blooms or concentrations were highest in the midsections of the Patuxent River (segments 10–30).

Mean phytoplankton concentrations were largely driven by these high concentrations in the shallower water between Nottingham and Lower Marlboro (see Lung and Bai 2003). In this region, phytoplankton growth may be flow limited (a flushing effect) in July through early September (Lung personal communication), which could account for the higher phytoplankton concentrations during the lowered nutrient loading scenario. In essence, phytoplankton biomass is flushed downriver under the higher flow, higher nutrient loading conditions. In the downstream, deeper parts of the Patuxent River, phytoplankton concentrations correlated with nutrient loadings for all seasons, but these small differences were not sufficient to compensate for the larger differences (and higher phytoplankton levels) upstream.

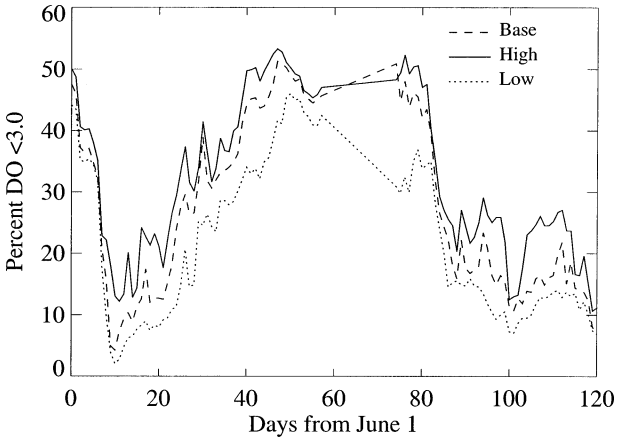

Fig. 3. Percent of the water volume with less than 3 mg l^{-1} of dissolved oxygen within the Patuxent River during low, baseline, and high nutrient loadings for all segments combined.

Menhaden Growth Rate Potential and Ecosystem Carrying Capacity

The bioenergetics model output of the specific rate of maximum consumption, metabolic losses, and scope for growth for a 10 g menhaden at different water temperatures is shown in Fig. 6. Men-

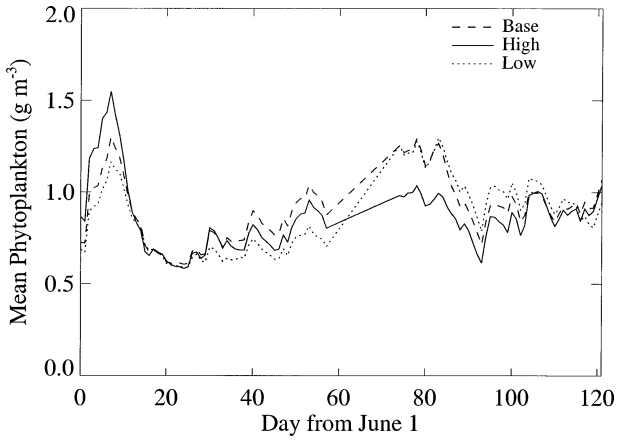

Fig. 4. Mean phytoplankton concentrations across the year under low, baseline, and high nutrient loadings for all segments combined.

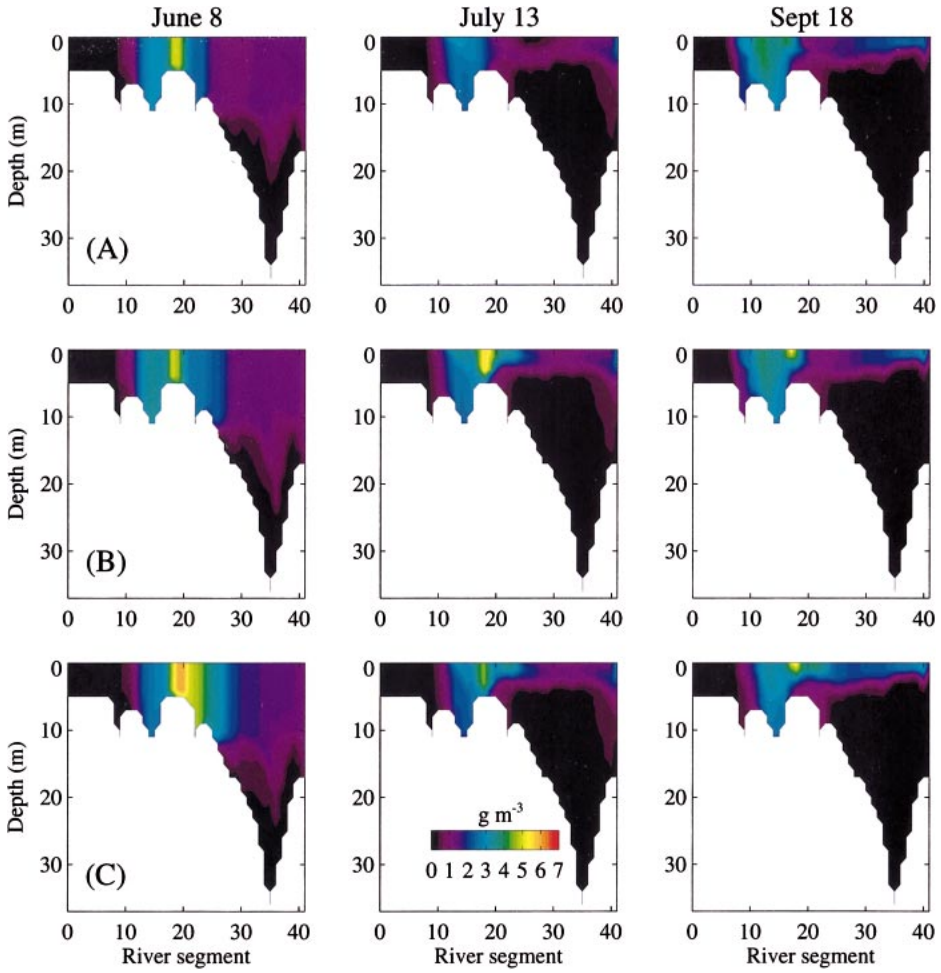

Fig. 5. Two-dimensional spatial distribution of phytoplankton concentrations on June 8, July 13, and September 18 down the axis of the Patuxent River during low (top row), baseline (middle row), and high (bottom row) nutrient loadings.

haden GRP (under maximum consumption) begins at about 14°C and increases relatively rapidly to 20–21°C. Menhaden have a broad area of relatively high consumption rates and scope for growth that ranges from about 21–30°C. Changes in temperatures within this range will have little effect on growth rates at high prey abundances. GRP falls off to zero near 32°C.

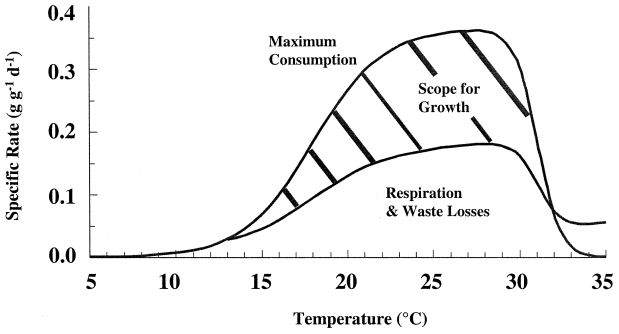

Fig. 6. Bioenergetics model output of the specific rates of maximum consumption, metabolic losses, and scope for growth for a 10 g menhaden at different water temperatures.

The 2-dimensional spatial distributions of menhaden GRP on June 8, July 13, and September 18 down the axis of the Patuxent River during low, baseline, and high nutrient loadings are shown in Fig. 7. To a large extent, the growth rate patterns followed those of phytoplankton because, during any one season, the temperature variation was low and menhaden growth response to temperatures varies little across a within-season temperature range (Fig. 6). Highest menhaden GRP occurred in the middle, shallower (< 5 m) stretches of the Patuxent River during all seasons, but shifted slightly upriver during September. Most of the growth was concentrated in the shallow (< 5 m) portions of the water column. In the downriver regions of the Patuxent River, menhaden GRP near-

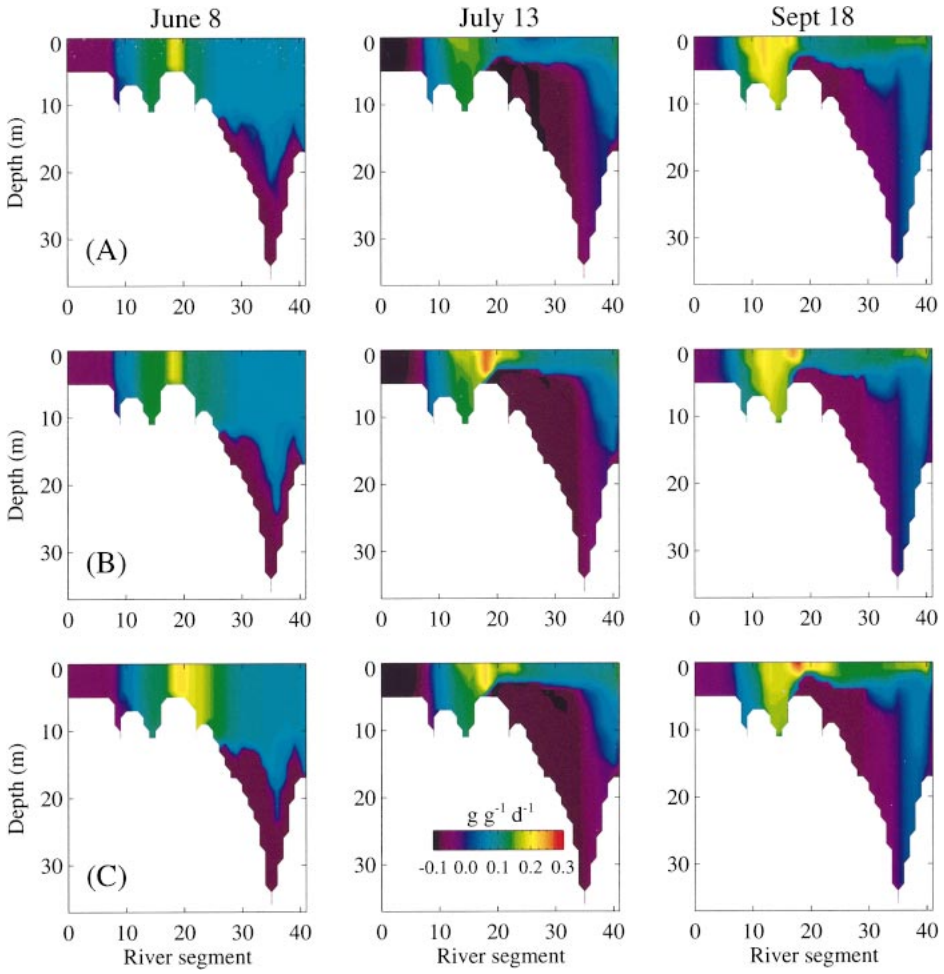

Fig. 7. Two-dimensional spatial distribution of menhaden growth rate potential on June 8, July 13, and September 18 down the axis of the Patuxent River during low (top row), baseline (middle row), and high (bottom row) nutrient loadings.

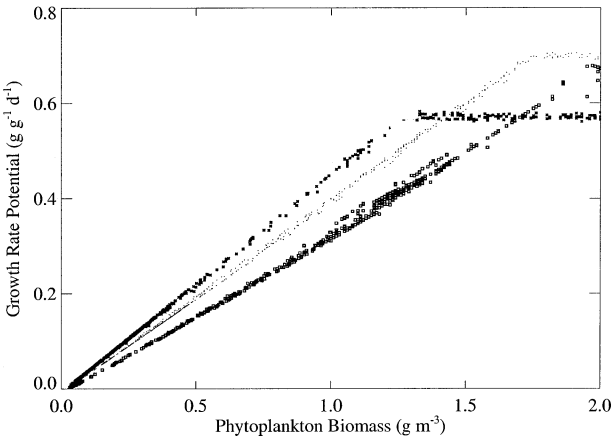

Fig. 8. Correlation of menhaden growth rate potential and phytoplankton concentrations for June 8 (open squares), July 13 (solid dots), and September 18 (solid squares).

er surface (< 5 m) increased slightly with increased nutrient loading during all seasons. In contrast, the areas of poorest growth (i.e., most weight loss) in deeper water was correlated with lowest oxygen levels.

Menhaden GRP was tightly and linearly related to phytoplankton concentrations within a season, but this relationship broke down under high phytoplankton concentrations when maximum consumption was reached (Fig. 8). The slope of the relationship was driven by prevailing temperatures (see Fig. 6). Hypoxic conditions inhibited feeding and thus growth in the model, but phytoplankton levels were not high in hypoxic water. Mean GRP varied as a function of time and land-use scenarios. For all three nutrient loadings, mean GRP had a spring peak, a broad time span of high growth in late summer (Fig. 9), and a third, slightly lower peak occurring around mid-July (days 40–55). These patterns in GRP followed those for phyto-

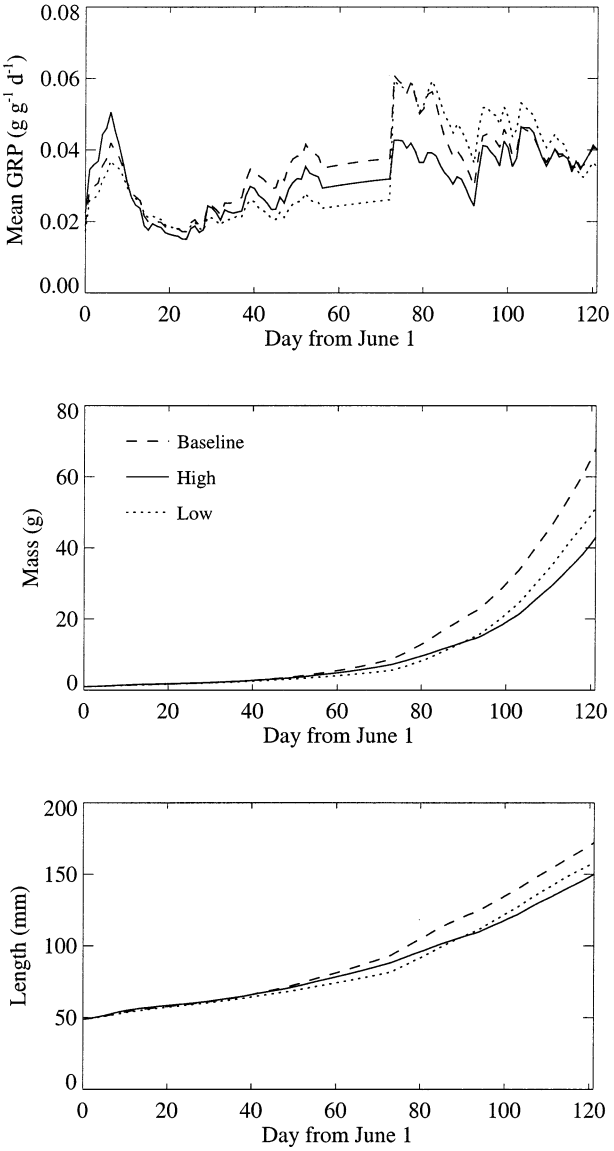

Fig. 9. Mean growth rate potential (top), mass (middle), and total length (bottom) of menhaden across the year under low, baseline, and high nutrient loadings for all segments combined.

plankton. Overall, the central shallow region of the Patuxent River contained relatively high concentrations of phytoplankton that supported high growth regions for menhaden.

Differences also occurred for mean GRP among land-use patterns (Fig. 9). In general, mean GRP for all three loading scenarios tracked similarly but with changes in the relative strength among the three. The low nutrient loading scenario resulted in lower mean GRP in the spring and early summer, but had the highest mean GRP in the late summer. In fact, the mean GRP for all three scenarios did a complete reversal from spring to late summer, where the mean GRP was highest at the lowest nutrient loading. The spring and late summer mean GRP tracked the mean phytoplankton concentrations suggesting that mean GRP was driven by regional patterns in phytoplankton concentrations. Consistent with these seasonal patterns between the three scenarios, mean GRP was positively related to nutrient loading in the spring, but negatively related in the late summer.

Menhaden biomass at the end of the growing season was 68 g under current nutrient loadings but only reached 51 g under reduced nutrient loadings. The lowest growth (43 g) was achieved under the highest nutrient loadings. Total lengths under baseline, reduced, and increased nutrient loadings were 172, 158, and 150 mm, respectively (Fig. 9).

Mean carrying capacity and percent of cells supporting positive carrying capacity, also varied as a function of time and nutrient loading. The carrying capacity varied widely across the season and from day to day (Fig. 10). In general, the highest nutrient loadings produced the lowest carrying capacity because many of the cells did not support growth.

Discussion

We examined how the quality and quantity of the pelagic habitat for menhaden changed in response to changes in land-use practices and nutrient loading. The models demonstrated that the habitat quality and quantity for menhaden will change with changes in land use but that the direction of the change and the time and space patterns of those changes are complex. Our modeling results suggest that land-use practices that lower the nutrient loadings to the Patuxent River would lower the overall GRP (and habitat quality) for Atlantic menhaden during June and in the lower portions of the river during other seasons. This is expected since menhaden growth rates are highly dependent on food availability and that phytoplankton biomass density is highly dependent on nutrient concentrations (e.g., Nixon 1981; Lung and Bai 2003). This was not always true. Our modeling exercise suggested that increased nutrient loadings above the baseline conditions as well as decreased nutrient loading could both cause a decrease in year-end growth of menhaden when averaged across the river. This was driven largely by changes in upriver phytoplankton patch densities, which were likely influenced by both nutrient concentrations and flow rates (Lung personal communication). Menhaden GRP was negative in deeper waters of the river during summer, particularly in hypoxic water.

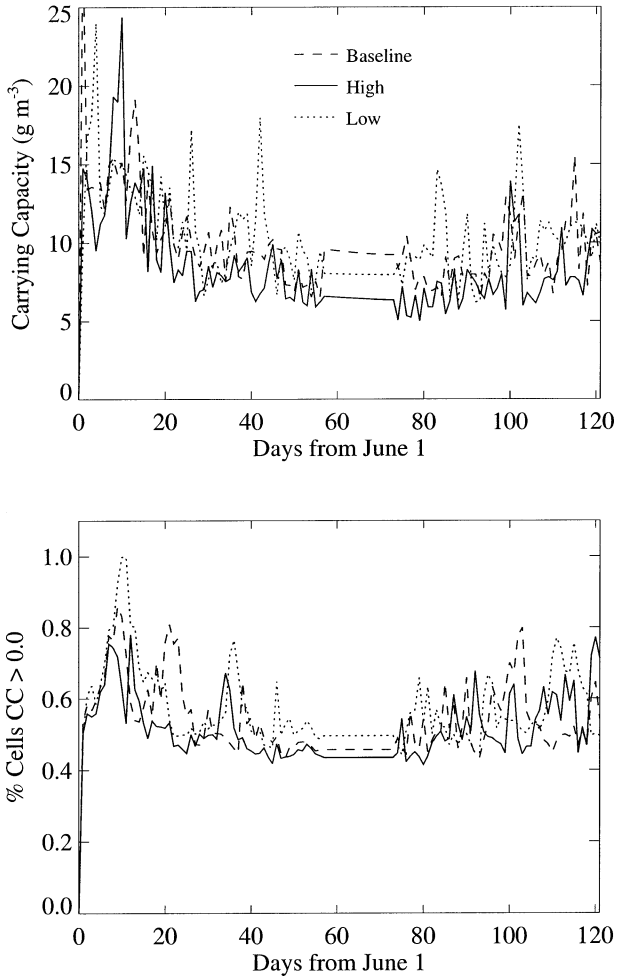

Fig. 10. Mean carrying capacity (top) and percent of cells with positive carrying capacity (bottom) of menhaden in the Patuxent River under low, baseline, and high nutrient loadings.

Results suggest that we clearly need to consider the spatial and temporal dynamics of the nutrient-phytoplankton-menhaden growth relationship. There were large spatial variations in habitat conditions for menhaden. Changes in nutrient loadings affected overall mean menhaden growth rates but the spatial arrangement and extent of regions for high, low, and medium menhaden growth rates changed with season and nutrient loadings. Menhaden growth rates have a nonlinear relationship with water temperatures and phytoplankton densities (combined) and overall results may be dependent on the specific seasonal temperature pattern. It is clear that single point estimators (in time or space) would not be a good indicator of menhaden habitat quality. This model could be tested by comparing modeled growth rates with observed growth rates and measured interannual variations in temperature, dissolved oxygen, and phytoplankton, if sufficient high-resolution spatial and temporal data were available.

Our results are dependent on a number of inherent assumptions in the models. Assumptions in the watershed model are discussed in Weller et al. (2003) and assumptions in the water quality model are discussed in Lung and Bai (2003). Many of the basic assumptions in the bioenergetics model and foraging model are discussed in Luo et al. (2001) and references cited therein. The fish foraging model was not directly linked to the water quality model and there was no feedback of menhaden predation on phytoplankton levels. Menhaden can cause local depletion of phytoplankton levels (D'Elia et al. 2003) but the extent of this depletion will depend directly on menhaden population densities. We also did not include other components of the food web such as zooplankton biomass, zooplankton predation on phytoplankton, and piscivore predation on menhaden and other important zooplanktivores such as bay anchovy, *Anchoa mitchelli* (e.g., Luo and Brandt 1993). Results will likely differ for different species of fish and may differ for menhaden when more components of the food web or food web dynamics are considered because of changes in consumption of phytoplankton by others. For example, White and Roman (1992) have shown that zooplankton grazing can consume 12–44% of the daily primary production in the Chesapeake Bay. We also assumed that menhaden fed exclusively on phytoplankton although some zooplankton is also ingested by filter-feeding menhaden (Keller et al. 1990).

The overall purpose of any modeling exercise should be to point out the areas where more information is needed. This paper clearly points out the need for more research in prediction of phytoplankton concentrations in time and space, menhaden foraging efficiency, and menhaden habitat selection if any quantitative predictions of how changes in land use affect menhaden production are to be made.

The importance of accurately predicting phytoplankton levels in time and space cannot be overestimated. For the pelagic menhaden, consumption and thus growth, is linearly correlated with phytoplankton density in time and space. Year-end growth rates are largely driven by mid summer phytoplankton concentrations (if we disregard mortality factors) because the temperature ranges in the Patuxent River during any one season are relatively small and the growth response of menhaden to temperature is broad and highest during late summer. The water quality model produced small dense patches of phytoplankton that largely dominated calculations of overall mean phytoplankton levels as well as caused patches of high menhaden growth rates.

The differences in phytoplankton densities in these patch areas were likely the result of both changes in nutrient loadings as well as changes in flow rates and produced counterintuitive results with respect to overall phytoplankton levels relative to nutrient loadings. This model output must be validated. The model results also demonstrate the importance of a monitoring program that samples at appropriate time and space scales to capture and characterize such patterns.

Research is also needed on menhaden foraging. There is little information on menhaden foraging efficiency and consumption rates for phytoplankton, particularly with respect to differences in water temperatures, oxygen levels, and phytoplankton densities. This type of information is clearly needed to move model predictions from a qualitative to a quantitative level. A sensitivity analysis on the foraging and bioenergetics models (Demers and Brandt unpublished data) found that the final weight of a menhaden at the end of the first growing season could differ by over 300% for a ± 10% change in foraging parameters. In contrast, ± 10% changes in metabolism, specific dynamic action, egestion, or excretion produced less than a 30% change in final weight. We assumed that lowered oxygen levels reduced consumption rates. This assumption needs testing.

Another important area for research concerns menhaden habitat selection. The spatial model of GRP provides information on the habitat afforded to a particular species. We need to understand how menhaden behaviorally respond to that environment if we want to predict the impact of changes in the environment on the population (e.g., Tyler and Brandt 2001). There is little information on menhaden habitat selection in the environment relative to water temperatures, oxygen concentrations, food availability, or GRP. Habitat selection will have a large effect on realized growth rates (e.g., Brandt 1993; Tyler and Brandt 2001). If menhaden selectively inhabit those regions that offer the best growth rates, or (for our simulations) have a completely random distribution, then higher or lower nutrient loadings would result in lower growth rates of menhaden in the Patuxent River as compared with baseline conditions. Year-end growth rate would be much higher if menhaden only occupied the regions of highest phytoplankton densities. If menhaden choose to occupy only the lower, deeper portions of the Patuxent River, then year-end size of menhaden may be more correlated with nutrient loading levels, but overall carrying capacity may be much lower. Little is known about the detailed spatial distribution of menhaden in the Chesapeake Bay. Some studies do suggest that menhaden are able to respond to gradients of phytoplankton biomass (Kemmerer 1980; Friedland et al. 1989, 1996). Under our assumption of random habitat selection, menhaden grew at rates comparable to those observed for menhaden in the Chesapeake Bay (20–60 g, Bonzek et al. 1992; Luo et al. 2001).

The changes in oxygen levels had relatively little impact on the menhaden growth rates. This might be expected for a pelagic species that relies on phytoplankton for food and would likely avoid hypoxic regions. If reduced oxygen somehow caused changes in phytoplankton densities through the food web, then menhaden growth rate could be affected. Results may differ with different species that are more dependent on benthic production. The extent of hypoxia, however, did affect carrying capacity by reducing the overall number of cells capable of supporting menhaden growth (Fig. 10).

The objective of this study was to link a fish growth rate model with a water quality model and to simulate how changes in land-use patterns might affect pelagic fishes. Menhaden were selected for this study because they are directly coupled to phytoplankton production, represent a pelagic species that has economic and ecological importance in estuaries along the Atlantic coast of the U.S., and allow for the evaluation on how changes in hypoxic and anoxic conditions, mediated through land-use practices, might impact pelagic fish habitat. These simulations are a first attempt at illustrating how changes in land-use patterns can affect fish habitat quality and will likely affect the ability of an estuary to serve as a nursery ground for important fishes. Despite the insight gained from our modeling exercise, there is clearly room for more research in directly linking hydrodynamic models, water quality models, and fish foraging, growth, and behavioral models.

Acknowledgments

This research was funded by the National Oceanic and Atmospheric Administration (NOAA) Coastal Ocean Programs multidisciplinary study of Complexity and Stressors in Estuarine Systems (COASTES) and the NOAA Great Lakes Environmental Research Laboratory. We thank Songzhi Liu and Laura Florence for help in programming and data analyses and W. Lung for use of his model output data. This is Great Lakes Environmental Research Laboratory contribution number 1263.

Literature Cited

Ahrenholz, D. W., W. R. Nelson, and S. P. Epperly. 1987. Population and fishery characteristics of Atlantic menhaden, *Brevoortia tyrannus*. *Fishery Bulletin U.S.* 85:569–600.

Baird, R. M. and R. E. Ulanowicz. 1989. The seasonal dynamics of the Chesapeake Bay ecosystem. *Ecological Monographs* 59: 329–364.

Bartell, S. M., J. E. Breck, R. H. Gardner, and A. L. Brenkert. 1986. Individual parameter perturbation and error analysis of fish bioenergetics models. *Canadian Journal of Fisheries and Aquatic Sciences* 43:160–168.

Bonzek, C. F., P. J. Gees, J. A. Colvocoresses, and R. E. Harris,

JR. 1992. Juvenile finish and blue crab assessment program. Virginia Institute of Marine Sciences Special Scientific Report Number 124. Gloucester Point, Virginia.

BRANDT, S. B. 1993. The effects of thermal fronts on fish growth: A bioenergetics evaluation of food and temperature. *Estuaries* 16:142–159.

BRANDT, S. B. AND K. J. HARTMAN. 1993. Innovative approaches with bioenergetics models: Future applications to fish ecology and management. *Transactions of the American Fisheries Society* 122:731–735.

BRANDT, S. B. AND J. KIRSCH. 1993. Spatially explicit models of striped bass growth in the mid-Chesapeake Bay. *Transactions of the American Fisheries Society* 122:845–869.

BRANDT, S. B., D. M. MASON, AND E. V. PATRICK. 1992. Spatially explicit models of fish growth rate. *Fisheries* 17:23–35.

CERCO, C. F. AND T. M. COLE. 1993. Three-dimensional eutrophication model of Chesapeake Bay. *Journal of Environmental Engineering* 119:1006–1025.

COLE, T. M. AND S. A. WELLS. 2000. CE-QUAL-W2: A two-dimensional lateral averaged, hydrodynamic and water quality model, Version 3. Instruction Report EL-2000-1. U.S. Army Engineering an Research Development Center, Vicksburg, Mississippi.

CRONIN, T. M. AND C. D. VANN. 2003. The sedimentary record of climatic and anthropogenic influence on the Patuxent estuary and Chesapeake Bay ecosystems. *Estuaries* 26:196–209.

D'ELIA, C. F., W. R. BOYNTON, AND J. G. SANDERS. 2003. A watershed perspective on nutrient enrichment, science, and policy in the Patuxent River, Maryland: 1960–2000. *Estuaries* 26: 171–185.

DURBIN, A. G. AND E. G. DURBIN. 1975. Grazing rates of the Atlantic menhaden *Brevoortia tyrannus* as a function of particle size and concentration. *Marine Biology* 33:265–277.

DURBIN, E. G. AND A. G. DURBIN. 1981. Assimilation efficiency and nitrogen excretion of a filter-feeding planktivore, the Atlantic menhaden, *Brevoortia tyrannus* (Pisces: Clupeidae). *Fisheries Bulletin U.S.* 79:601–616.

FRIEDLAND, K. D., D. W. AHRENHOLZ, AND J. F. GUTHRIE. 1989. Influence of plankton on distribution patterns of the filter feeder *Brevoortia tyrannus* (Pisces: Clupeidae). *Marine Ecology Progress Series* 54:1–11.

FRIEDLAND, K. D., D. W. AHRENHOLZ, AND J. F. GUTHRIE. 1996. Formation and seasonal evolution of Atlantic menhaden juvenile nurseries in coastal estuaries. *Estuaries* 19:105–114.

FRIEDLAND, K. D., L. W. HAAS, AND J. V. MERRINER. 1984. Filtering rates of the juvenile Atlantic menhaden *Brevoortia tyrannus* (Pisces: Clupeidae), with consideration of the effects of detritus and swimming speed. *Marine Biology* 84:109–117.

HARTMAN, K. J. AND S. B. BRANDT. 1995. Trophic resource partitioning, diets, and growth of sympatric estuarine predators. *Transactions of the American Fisheries Society* 124:520–537.

HILDEBRAND, S. F. AND W. C. SCHROEDER. 1928. Fishes of Chesapeake Bay. *U.S. Bureau of Fisheries Bulletin* 43:1–388.

JORDAN, T. E., D. E. WELLER, AND D. L. CORRELL. 2003. Sources of nutrient inputs to the Patuxent River estuary. *Estuaries* 26: 226–243.

JUNE, F. C. AND F. T. CARLSON. 1971. Food of young Atlantic menhaden, *Brevoortia tyrannus,* in relation to metamorphosis. *Fisheries Bulletin U.S.* 68:493–512.

KELLER, A. A., P. H. DOERING, S. P. KELLY, AND B. K. SULLIVAN. 1990. Growth of juvenile Atlantic menhaden *Brevoortia tyrannus* (Pisces: Clupeidae), in MERL mesocosms: Effects of eutrophication. *Limnology and Oceanography* 35:109–122.

KEMMERER, A. J. 1980. Environmental preferences and behavior patterns of gulf menhaden (*Brevoortia patronus*) inferred from fishing and remotely sensed data, p. 345–370. *In* J. E. Bardach, J. J. Magnuson, R. C. May, and M. J. Reinhart (eds.), Fish Behavior and Its Uses in the Capture and Culture of Fishes. ICLARM Conference Proceedings, Volume 5. International Center for Living Aquatic Resources Management, Manila, Philippines.

KITCHELL, J. F., D. J. STEWART, AND D. WEININGER. 1977. Applications of a bioenergetics model to yellow perch (*Perca flavescens*) and walleye (*Stizostedion vitreum vitreum*). *Journal of the Fisheries Research Board of Canada* 34:1922–1935.

LEWIS, V. P. AND D. S. PETERS. 1984. Menhaden-A single step from vascular plant to fishery harvest. *Journal of Experimental Marine Biology and Ecology* 84:95–100.

LUNG, W. S. AND S. BAI. 2003. A water quality model for the Patuxent estuary: Current conditions and predictions under changing land-use scenarios. *Estuaries* 26:267–279.

LUO, J. AND S. B. BRANDT. 1993. Bay anchovy, *Anchoa mitchilli,* production and consumption in mid-Chesapeake Bay based on a bioenergetics model and acoustical measures of fish abundance. *Marine Ecology Progress Series* 98:223–236.

LUO, J., K. J. HARTMAN, S. B. BRANDT, C. F. CERCO, AND T. H. RIPPETOE. 2001. A spatially-explicit approach for estimating carrying capacity: An application for the Atlantic Menhaden (*Brevoortia tyrannus*) in Chesapeake Bay. *Estuaries* 24:545–556.

NIXON, S. W. 1981. Freshwater inputs and estuarine productivity, p. 31–57. *In* R. D. Cross and D. L. Williams (eds.), Proceedings of the National Symposium on Freshwater Inflow to Estuaries, Volume 1. FWS/OBS-81/04. U.S. Fish and Wildlife Service, Office of Biological Service, Washington, D.C.

PETERS, D. S. AND W. E. SCHAFF. 1981. Food requirements and sources for juvenile Atlantic menhaden. *Transactions of the American Fisheries Society* 110:317–324.

PETERS, D. S. AND W. E. SCHAFF. 1991. Empirical model of the trophic basis for fishery yield in coast waters of the eastern USA. *Transactions of the American Fisheries Society* 120:459–473.

QUINLAN, J. A. AND L. B. CROWDER. 1999. Searching for sensitivity in the life history of Atlantic menhaden: Inferences from a matrix model. *Fisheries Oceanography* 82:124–133.

RIPPETOE, T. H. 1993. Production and energetics of Atlantic menhaden in Chesapeake Bay. M.S. Thesis, University of Maryland, College Park, Maryland.

SMITH, J. W. 1999. Distribution of Atlantic Menhaden, *Brevoortia tyrannus* purse-seine sets and catches from southern New England to North Carolina, 1985–96. Technical report NMFS 144. National Oceanic and Atmospheric Administration, Beaufort, North Carolina.

THORTON, K. W. AND A. S. LESSEM. 1978. A temperature algorithm for modifying biological rates. *Transactions of the American Fisheries Society* 107:284–287.

TYLER, J. A. AND S. B. BRANDT. 2001. Do spatial models of growth rate potential reflect fish growth in a heterogeneous environment? A comparison of model results. *Ecology of Freshwater Fish* 10:43–56.

U.S. NATIONAL MARINE FISHERIES SERVICE (NMFS). 1978. Fishery statistics of the United States, 1977. U.S. National Marine Fisheries Service Current Fisheries Statistics, No. 7500. Silver Springs, Maryland.

WARLEN, S. M. 1994. Spawning time and recruitment dynamics of larval Atlantic menhaden, *Brevoortia tyrannus,* into a North Carolina estuary. *Fisheries Bulletin U.S.* 92:420–433.

WELLER, D. E., T. E. JORDAN, D. L. CORRELL, AND Z.-J. LIU. 2003. Effects of land-use change on nutrient discharges from the Patuxent River watershed. *Estuaries* 26:244–266.

WHITE, J. R. AND M. R. ROMAN. 1992. Seasonal study of grazing by metazoan zooplankton in the mesohaline Chesapeake Bay. *Marine Ecology Progress Series* 86:251–261.

SOURCE OF UNPUBLISHED MATERIALS

DEMERS, E. unpublished data. Malaspina University-College, Nanaimo, British Columbia, Canada.

Received for consideration, June 5, 2002
Revised, January 8, 2003
Accepted for publication, January 22, 2003